

MONABIPHOT

Master Thesis

Óscar Andrés NAJERA OCAMPO
najera.oscar@gmail.com

Study of spin-orbit coupling in the metal-Mott insulator transition

HOST INSTITUTION

Université Paris-Sud
15 Rue Georges Clemenceau, 91400 Orsay

Laboratoire de Physique de Solides - Theory Group
<https://www.lps.u-psud.fr/>

ADVISERS:

- Rozenberg Marcello
marcelo.rozenberg@u-psud.fr
- Civelli Marcello
marcello.civelli@u-psud.fr

Defence date:

Acknowledgements

I would like to thank my advisers Marcello Civelli and Marcello Rozenberg for their kind support during the development of this work and also for welcoming me into the theory group at LPS-Orsay. I would also like to thank Sergueï Tchoumakov for the exiting discussions we shared within the office, allowing us to better understand our own work.

Abstract

The spin-orbit interaction, although usually considered as a small relativistic correction in the discussion of electrons in solids, has shown to be able to drive systems into new states of matter, like the topological insulators, whose nature has remained unnoticed up to now. An interesting question, recently arising in the context of $5d$ -electron system (like Sr_2IrO_4), is whether the spin-orbit interaction may also act in conjunction or competition with the Mott strong correlation and determine unusual ground-state properties.

In this work a three-orbital Hubbard model is taken as playground to study $5d$ -electron physics. The phase-diagram as a function of the spin-orbit interaction and electronic correlation is mapped within the framework of the slave-spins mean-field approximation. The outcoming behavior is compared to the physical behavior of Sr_2IrO_4 and Sr_2RhO_4 .

Contents

1	Introduction: Spin-orbit interaction meets strong correlation	3
2	Theoretical aspects	4
2.1	The Hubbard Model	4
2.2	Spin-orbit interaction	5
3	Method: Slave Spin Mean Field	7
3.1	Introductory Idea	7
3.1.1	Isolated Atom	8
3.2	The lattice model	9
3.2.1	New operator's representation	10
3.2.2	Single-site mean field approximation	11
3.2.3	The choice of the c parameter	13
3.3	Spin-orbit Interaction	14
4	Results	16
4.1	Half filled multi-band case	17
4.2	Doping the systems	18
4.3	Spin orbit interaction	19
4.4	Weaknesses of the method	25
5	Conclusions and future work	27
A	Slave spin method modifications	30

Chapter 1

Introduction: Spin-orbit interaction meets strong correlation

Transition metal oxides have dominated materials research in the past decades. Unusual properties have been most extensively studied in d -electron systems, particularly motivated by phenomena like high- T_c superconductivity in cuprates and colossal magnetoresistance in manganites[1].

Especially important are the transitions driven by correlation effects associated with electron-electron interaction, leading to metal-insulator transitions. The insulating phase caused by correlation effects, that results from a strong local Coulomb repulsion among the charge carriers, is categorized as the Mott Insulator. The physics of Mott insulators remains at the center of condensed matter physics. On the other hand the spin-orbit interaction, though well understood in the context of semiconductors and considered as a small relativistic correction to the Schrödinger equation, is capable of driving systems into novel states of matter that have remained unnoticed up to very recently. This has led into research activity of topological insulators, which are standard band insulators in the bulk but present metallic edge states at the surface.

These two research strands come together in the heavy transition metal compounds drawn especially from the $5d$ series, and in some cases the $4d$ series as well. Upon descending the periodic table from the $3d$ to $4d$ to the $5d$ series, there are several competing trends. First, the d orbitals become more extended, tending to reduce the local electronic repulsion (U) and thereby diminish correlation effects. However, simultaneously, the spin-orbit coupling increases dramatically, leading to enhanced energy levels splittings between otherwise degenerate or nearly degenerate orbitals and bands, reducing in many cases the kinetic energy of electrons. The latter effect can allow for correlation physics to come into play. An increasing number of experiments in the recent years focuses into this correlated-spin-orbit-coupling regime. Most prolific are a collection of *iridates*, weakly conducting or insulating oxides containing iridium, primarily in the Ir^{4+} oxidation state. These compounds have revealed thermal phase transitions, an evolution from metallic to insulating states, and a large systematic variation of their properties. Many theoretical ideas have also been introduced in this context, like topological Mott insulators, chiral spin liquids and Weyl semi-metals[2].

It becomes an interesting question to investigate how this interactions change the nature of the correlated material, if their interplay is cooperative or competitive with the spin-orbit interaction in generating insulating states and explore this new exotic phases of matter.

Chapter 2

Theoretical aspects

2.1 The Hubbard Model

From the theoretical point of view, a minimal model Hamiltonian that considers the competition between the delocalized nature of electrons in a solid due to the periodic potential from the lattice, and the localization tendency produced by electronic interactions is the (single-band) Hubbard model, which reads:

$$\mathcal{H} = -t \sum_{\langle i,j \rangle, \sigma} c_{i\sigma}^\dagger c_{j\sigma} + U \sum_i n_{i\uparrow} n_{i\downarrow} \quad (2.1)$$

where t is the hopping amplitude between lattice sites, $\langle i, j \rangle$ denotes the first neighbors pairs of sites in the lattice, $(c_{i\sigma}^\dagger, c_{i\sigma})$ are the creation and annihilation operators of an electron on site i and with spin σ , U is the local Coulomb repulsion and $n_{i\sigma}$ is the number operator on site i and with spin σ . A pictorial representation of this model can be seen in figure 2.1a. The first term of the Hamiltonian (2.1) is the Tight-Binding term, it enables electrons to hop between lattice sites gaining kinetic energy. This promotes their delocalization in the periodic potential of the lattice and gives the metallic behavior. The results is a delocalized electron sea, called Fermi sea, as illustrated in figure 2.1b. On the other hand, if the double occupation of a lattice site is severely penalized by the local coulomb repulsion(U), the second term in the Hamiltonian (2.1), electrons prefer to localize themselves and single occupy each lattice site. This is the behavior depicted in figure 2.1c, the Mott insulator. The difficulty on solving this problem, which remains unsolved up to present days apart from the one- and infinite-dimensions case, essentially comes from the non-commutativity of the first term, which is diagonal in momentum

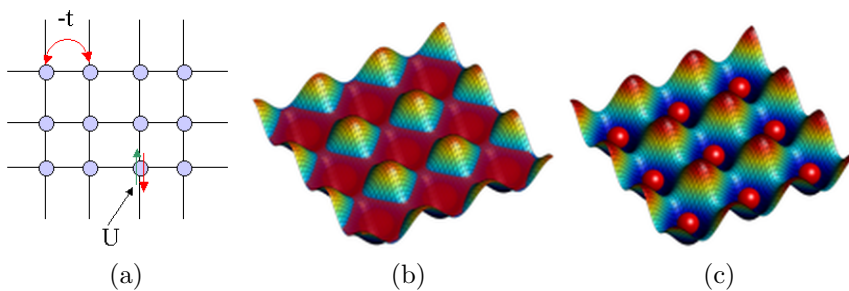


Figure 2.1: a) Lattice illustration of the Hubbard model b) Delocalized electrons forming a metal c) Localized electrons forming a Mott insulator

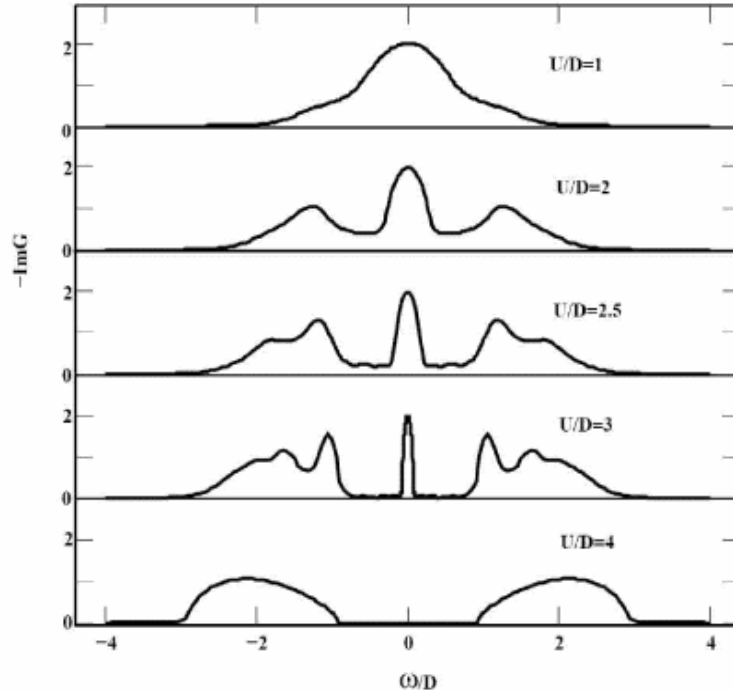


Figure 2.2: Spectral function for several values of the interaction strength in DMFT for the half-filled Hubbard model[3]

space, and the local interaction term which is diagonal in real space. Furthermore, when the strengths of both terms are comparable it is not possible to use perturbation theory.

The Hubbard problem has been very well studied in the infinite dimensions limit, within the framework of the dynamical mean-field theory(DMFT)[3]. In figure 2.2 we show plots of the spectral function of the half-filled (where the average site occupancy is 1 electron) Hubbard model. In the metallic state, at low interaction values($U/D = 1$) there is a single half-filled conducting band. When interactions are increased spectral weight is transferred from low energy to higher energy(of the order of U/D). Upper and Lower Hubbard bands start to form, as well as the quasiparticle peak at the Fermi level showing the well known 3 peaks density of states. By further increasing the interaction the quasiparticle peak is narrowed until disappearance at high local interactions and the system is driven into the Mott insulator state. A gap of the order of U/D (in the strong U limit) opens around the Fermi level, leaving only 2 Hubbard bands. Only the lower Hubbard band is occupied.

2.2 Spin-orbit interaction

The spin-orbit interaction becomes relevant in heavy elements (the strength of the spin-orbit coupling increases proportionally to the fourth power of the atomic number of the atom $\zeta \sim Z_a^4$) leading to non-trivial topological phenomena. This seems to be the case for the heavy transition metal compounds especially from the $5d$ series, where the spin-orbit interaction becomes relevant and shows and interplay with the strong correlation typical of d orbitals.

The Spin-orbit interaction arises because the magnetic moment associated with the

electron's spin interacts with the orbital motion of the electron in an atom. In the electron reference frame the orbital motion represents a magnetic field to which the electron tends to line up with its own magnetic moment. This interaction is included to the atomic Hamiltonian as a term like[4]:

$$\mathcal{H}'_{SO_{atom}} = \zeta(r)\mathbf{L} \cdot \mathbf{S} \quad (2.2)$$

where $\zeta(r)$ is the strength of the spin-orbit interaction, \mathbf{L} is the orbital angular momentum operator and \mathbf{S} is the spin operator. Since the interaction couples the operators \mathbf{L} and \mathbf{S} in the Hamiltonian $\mathcal{H}'_{SO_{atom}}$ the magnetic m_ℓ and the electron spin quantum numbers are no longer good quantum numbers. Therefore one introduces the total angular momentum operator $\mathbf{J} = \mathbf{L} + \mathbf{S}$, which commutes with the spin-orbit interaction (2.2) and introduces the new quantum numbers j and m_j . To find the magnitude of the spin-orbit interaction, one takes the matrix elements of $\mathcal{H}'_{SO_{atom}}$ in the representation $|j, \ell, s, m_j\rangle$. For this one first takes the diagonal matrix elements of $\mathbf{J} \cdot \mathbf{J}$

$$\mathbf{J} \cdot \mathbf{J} = (\mathbf{L} + \mathbf{S}) \cdot (\mathbf{L} + \mathbf{S}) = \mathbf{L} \cdot \mathbf{L} + \mathbf{S} \cdot \mathbf{S} + 2\mathbf{L} \cdot \mathbf{S} \quad (2.3)$$

where the operators \mathbf{L} and \mathbf{S} commute since they operate in different coordinate spaces. So that the expected value of $\mathbf{L} \cdot \mathbf{S}$ in the $|j, \ell, s, m_j\rangle$ representation becomes¹:

$$\langle \mathbf{L} \cdot \mathbf{S} \rangle = \frac{1}{2}[j(j+1) - l(l+1) - s(s+1)] \quad (2.4)$$

As a short example, an electron in a p orbital has $\ell = 1$ and $s = 1/2$. So that its total angular momentum is $j = |l + s| = 3/2$ or $j = |l - s| = 1/2$. Using the above relation (2.4), to calculate the expected value of $\langle \mathbf{L} \cdot \mathbf{S} \rangle$, one obtains:

$$\langle \mathbf{L} \cdot \mathbf{S} \rangle = 1/2 \quad \text{for} \quad j = 3/2 \quad (2.5a)$$

$$\langle \mathbf{L} \cdot \mathbf{S} \rangle = -1 \quad \text{for} \quad j = 1/2 \quad (2.5b)$$

where the first level (2.5a) forms a quadruplet with isospins values of $m_j = -3/2, -1/2, 1/2, 3/2$ and the lower level forms a doublet with isospins values of $m_j = -1/2, 1/2$.

¹Here one considers a unit system where $\hbar = 1$

Chapter 3

Method: Slave Spin Mean Field

3.1 Introductory Idea

The resolution of the Hubbard Hamiltonian requires approximations. Many techniques have been proposed to deal with it, each presenting advantages and shortcomings. In this work, we shall employ a slave particle scheme: the slave spins technique[5]. This representation has the advantages of being computationally inexpensive, orbital selective and it allows the possibility to dope the system and drive it away from half-filling[6].

The idea in a slave particle scheme is to express the real fermion in terms of constrained(slave) auxiliary fields that enlarge the Hilbert space. These fields are subject to local restrictions that eliminate nonphysical states. In the slave spin case one starts from the observation that the possible occupancies of a real fermion(d) on a given site, $n_d = 0$ and $n_d = 1$, can be represented as two possible states of a spin-1/2 variable, $S^z = -1/2$ and $S^z = +1/2$. The idea then is to split the original particle into a spin-like degree of freedom and charge degree of freedom by introducing a spin-field and an associated auxiliary fermion(f). In this manner vacuum state and occupied states are represented as:

$$|\emptyset\rangle_d \equiv |n_f = 0, S^z = -1/2\rangle \quad (3.1a)$$

$$|1\rangle_d = d^\dagger |\emptyset\rangle_d \equiv |n_f = 1, S^z = +1/2\rangle \quad (3.1b)$$

In this context, the anti-commutation properties of the original fermion operator d are insured by the introduction of the auxiliary fermion operator f . Then, one formulates the constrain:

$$f^\dagger f = S^z + \frac{1}{2} \quad (3.2)$$

which insures that the number of auxiliary fermions and the spin's states are the same and, above all, it eliminates the nonphysical states

$$|n_f = 1, S^z = -1/2\rangle$$

$$|n_f = 0, S^z = +1/2\rangle$$

It is important to note that the spin-1/2 variable has nothing to do with the actual spin of the particle. The slave spin-1/2 variable is introduced for every fermion species to indicate (or not) the presence of the particle. Therefore, the original particle d_σ spin label σ has to be carried into the slave variables to label them with the same index:

$n_{f\sigma}$ and S_σ^z . For example, the single-orbital base $\{|\emptyset\rangle_d, |\uparrow\rangle_d, |\downarrow\rangle_d, |\uparrow\downarrow\rangle_d\}$ is represented in this slave-spin extended Hilbert space as:

$$|\emptyset\rangle_d \equiv |n_{f\uparrow} = 0; S_\uparrow^z = -1/2\rangle |n_{f\downarrow} = 0; S_\downarrow^z = -1/2\rangle \quad (3.3a)$$

$$|\uparrow\rangle_d \equiv |n_{f\uparrow} = 1; S_\uparrow^z = 1/2\rangle |n_{f\downarrow} = 0; S_\downarrow^z = -1/2\rangle \quad (3.3b)$$

$$|\downarrow\rangle_d \equiv |n_{f\uparrow} = 0; S_\uparrow^z = -1/2\rangle |n_{f\downarrow} = 1; S_\downarrow^z = 1/2\rangle \quad (3.3c)$$

$$|\uparrow\downarrow\rangle_d \equiv |n_{f\uparrow} = 1; S_\uparrow^z = 1/2\rangle |n_{f\downarrow} = 1; S_\downarrow^z = 1/2\rangle \quad (3.3d)$$

In an N -orbital system, $2N$ new spin-1/2 variables $S_{m\sigma}^z$ and $2N$ auxiliary fermions $f_{m\sigma}$ are introduced, where $m = 1, \dots, N$ is the orbital quantum number.

3.1.1 Isolated Atom

In order to test the slave-spin method, we first consider the case of a degenerate multi-orbital atom, whose analytical solution is well known. The Hamiltonian in particle-hole symmetry formulation reads:

$$\mathcal{H} = \frac{U}{2} \left(\sum_n d_n^\dagger d_n - N \right)^2 - \mu \sum_n d_n^\dagger d_n \quad (3.4)$$

The first step is to recast the Hamiltonian in terms of the new slave-spin operators. The first choice is to use the auxiliary fermions for the non-interacting term ($d_n^\dagger d_n \rightarrow f_n^\dagger f_n$) and the slave spins for the interacting case ($d_n^\dagger d_n \rightarrow S_n^z + \frac{1}{2}$). We seek a paramagnetic solution, then the constraint (3.2) which avoids nonphysical states is included through a unique Lagrange multiplier λ , since all particles are indistinguishable in spin and orbital quantum numbers. After this treatment the Hamiltonian reads:

$$\mathcal{H} = \frac{U}{2} \left(\sum_n S_n^z \right)^2 + \lambda \sum_n \left(S_n^z + \frac{1}{2} - f_n^\dagger f_n \right) - \mu \sum_n f_n^\dagger f_n \quad (3.5)$$

which is possible to separate into a fermion and a spin Hamiltonians:

$$\mathcal{H}_f = -(\lambda + \mu) \sum_n f_n^\dagger f_n \quad (3.6a)$$

$$\mathcal{H}_s = \frac{U}{2} \left(\sum_n S_n^z \right)^2 + \lambda \sum_n \left(S_n^z + \frac{1}{2} \right) \quad (3.6b)$$

The Lagrange multiplier λ is fixed at the mean-field level by determining the stationary point of the mean-field averaged Hamiltonian: $0 = \frac{\partial \langle \mathcal{H} \rangle}{\partial \lambda}$. Within this approach, the restriction (3.2) is therefore respected at the mean field level too.

$$\begin{aligned} 0 &= - \sum_n \langle f_n^\dagger f_n \rangle_f + \sum_n \langle S_n^z + \frac{1}{2} \rangle_s \\ 2Nn_F(-\lambda - \mu) &= 2N \langle S_n^z + \frac{1}{2} \rangle_s \equiv \langle Q \rangle_s \\ 2Nn_F(-\lambda - \mu) &= \mathcal{Z}^{-1} \sum_{Q=0}^{2N} \binom{2N}{Q} Q \exp(\beta(U/2(Q - N)^2 + \lambda Q)) \end{aligned} \quad (3.7)$$

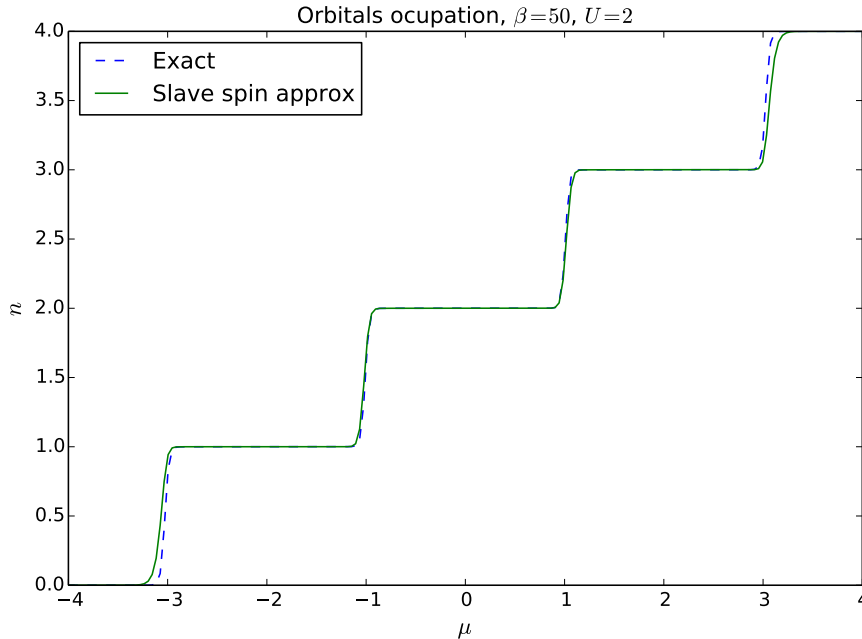


Figure 3.1: Filling vs chemical potential for a two degenerate orbital system in the atomic limit, within the slave spin representation and the exact result.

Averages are self-consistently performed with respect to their corresponding fermion and spin Hamiltonians (3.6), n_F is the Fermi distribution and

$$\mathcal{Z} = \sum_{Q=0}^{2N} \binom{2N}{Q} \exp(\beta(U/2(Q-N)^2 + \lambda Q))$$

is the Grand Canonical Partition function of the spin Hamiltonian (3.6b). Here $Q \leftarrow S + 1/2$ represents the charge in the system. By numerical solving the above equation (3.7), we can self-consistently determine the multiplier $\bar{\lambda}(\mu, \beta)$ and obtain the mean fermion occupation, $2N n_F(-\mu - \bar{\lambda}(\mu, \beta))$. The solution that we find can be conveniently represented by the total fermion occupation as a function of the chemical potential μ . The resulting curve displays the well known Coulomb ladder-shape (figure 3.1), where the system acquires only integer fillings. The change from an integer occupation to an adjacent one takes place abruptly as a function of the chemical potential μ .

It is necessary to compare the slave spins solution to the exact solution, given by:

$$2N \langle d^\dagger d \rangle = \mathcal{Z}^{-1} \sum_{Q=0}^{2N} \binom{2N}{Q} Q e^{\beta(U/2(Q-N)^2 - \mu Q)} \quad (3.8)$$

As seen in (figure 3.1), the slave spin approximation is capable of representing up to a good approximation the exact solution and it works best around half-filling.

3.2 The lattice model

Atoms on a lattice have overlapping orbitals and electrons are capable of moving from atom to atom, gaining kinetic energy. One can extend the previous atomic Hamiltonian

to include the Tight-Binding term to allow the electron motion on a lattice, so to obtain a multi-band Hubbard model, which reads:

$$\mathcal{H} = - \sum_m t_m \sum_{\langle i,j \rangle, \sigma} (d_{im\sigma}^\dagger d_{jm\sigma} + h.c.) + \sum_{im\sigma} (\epsilon_m - \mu) d_{im\sigma}^\dagger d_{im\sigma} + \frac{U}{2} \sum_i \left(\sum_{m\sigma} d_{im\sigma}^\dagger d_{im\sigma} - N \right)^2 \quad (3.9)$$

where t_m is the orbital specific hopping amplitude between sites, $\langle i, j \rangle$ denotes the first neighbors pairs in the given lattice dimension and geometry and ϵ_m is the orbital energy.

3.2.1 New operator's representation

When rewriting the Hamiltonian into the slave spin representation the electron number operators $d_{im\sigma}^\dagger d_{im\sigma}$ are expressed in terms of the auxiliary fermions and the slave spins fields exactly in the same way as done in the previous section 3.1.1, respecting all the quantum numbers i, m, σ . Nevertheless, the Tight-Binding part of the Hamiltonian (3.9) includes non-diagonal operators, and the change of representation has to be treated carefully. There is some freedom associated to this choice, since different operators in the enlarged Hilbert space spanned by the slave-spin and auxiliary fermions can have the same action on the physical Hilbert space. The trivial choice $d^\dagger \rightarrow S^+ f^\dagger$, $d \rightarrow S^- f$, although correct in the physical Hilbert space leads under further mean-field approximations to a problem with spectral weight conservation because S^+ and S^- don't commute. Instead the representation $d^\dagger \rightarrow 2S^x f^\dagger$ and $d \rightarrow 2S^x f$ is identical on the physical Hilbert space and involves commuting slave spin operators[5, 7].

Nevertheless the previously stated representation is not well suited for systems away of half-filling[7]. The quasiparticle residue will be associated with the quantity $Z_m = 4\langle S_{im\sigma}^x \rangle^2$, but for an isolated spin-1/2 particle the following equality holds:

$$\langle S^x \rangle^2 + \langle S^y \rangle^2 + \langle S^z \rangle^2 = \frac{1}{4} \quad (3.10)$$

Together with the slave-spin constrain (3.2) which is taken at the mean field level, we arrive to the inequality:

$$Z_m = 4\langle S_{im\sigma}^x \rangle^2 \leq 1 - 4\left(n - \frac{1}{2}\right)^2 \quad (3.11)$$

This shows the impossibility of Z to arrive to the unitary value in cases away of half-filling. In order to fix this, there is the need to search into a more general case for the selected operators. One starts with: ($d^\dagger \rightarrow O^\dagger f^\dagger$; $d \rightarrow O f$), in which O is a generic spin-1/2 operator. This operator will be determined by following the action of the real creation and annihilation operators (d^\dagger, d) over the real states. So that this new operator has the same effect into the extended Hilbert space of spin. We have in fact in the real physical space:

$$d|\emptyset\rangle = 0 \quad d^\dagger|1\rangle = 0 \quad (3.12a)$$

$$d|1\rangle = |\emptyset\rangle \quad d^\dagger|\emptyset\rangle = |1\rangle \quad (3.12b)$$

The first set of conditions (3.12a) can be assured by the fermion operator, the O operator does not play any role.

$$\begin{aligned} fO |n^f = 0, S^z = -\frac{1}{2}\rangle &= 0 \\ f^\dagger O^\dagger |n^f = 1, S^z = +\frac{1}{2}\rangle &= 0 \end{aligned}$$

Imposing the second set of conditions (3.12b)

$$\begin{aligned} fO |n^f = 1, S^z = +\frac{1}{2}\rangle &= |n^f = 0, S^z = -\frac{1}{2}\rangle \\ f^\dagger O^\dagger |n^f = 0, S^z = -\frac{1}{2}\rangle &= |n^f = 1, S^z = +\frac{1}{2}\rangle \end{aligned}$$

only three out of four matrix elements of the most general 2×2 matrix form of the O operator can be determined, and this implies that an unknown parameter c remains to be determined. The explicit matrix form of the (O, O^\dagger) operators in the $S^z = \pm 1/2$ basis $|+\rangle = \begin{pmatrix} 1 \\ 0 \end{pmatrix}$ & $|-\rangle = \begin{pmatrix} 0 \\ 1 \end{pmatrix}$ is given by [6]:

$$O = \begin{pmatrix} 0 & c \\ 1 & 0 \end{pmatrix} \quad O^\dagger = \begin{pmatrix} 0 & 1 \\ \bar{c} & 0 \end{pmatrix} \quad (3.13)$$

The O^\dagger operator (3.13) is then clearly expressed in terms of rising and lowering operators as $O^\dagger = S^+ + cS^-$. This stems from the fact that different operators can have the same effect in the physical subspace of the enlarged Hilbert space, while acting differently over nonphysical states. The enlarged spin system needs to allow for fluctuations in their internal degrees of freedom including the non physical states. It is then projection onto the physical space enforced by the restriction (3.2) that allows to follow the real system's dynamics.

Finally replacing the operators and enforcing the constrain (3.2) individually to every particle, respecting its lattice site, orbital and spin quantum numbers, one can reformulate the Hamiltonian (3.9) within the slave spin approximation as:

$$\begin{aligned} \mathcal{H} = & - \sum_m t_m \sum_{\langle ij \rangle, \sigma} (O_{im\sigma}^\dagger O_{jm\sigma} f_{im\sigma}^\dagger f_{jm\sigma} + h.c.) + \sum_{im\sigma} (\epsilon_m - \mu) f_{im\sigma}^\dagger f_{im\sigma} \\ & + \sum_{im\sigma} \lambda_{im\sigma} (S_{im\sigma}^z + \frac{1}{2} - f_{im\sigma}^\dagger f_{im\sigma}) + \frac{U}{2} \sum_i \left(\sum_{m\sigma} S_{im\sigma}^z \right)^2 \end{aligned} \quad (3.14)$$

3.2.2 Single-site mean field approximation

Approximations will now be introduced to treat the proposed Hamiltonian (3.14). First, the local constrains enforced by the Lagrange multipliers ($\lambda_{im\sigma}$) will be treated at mean-field level, analogously to section 3.1.1 using the condition $\nabla_\lambda \langle \mathcal{H} \rangle = 0$ under the assumption that the Lagrange multipliers are static and site-independent $\lambda_{m\sigma}$.

The second approximation consists of decoupling the auxiliary fermions and slave spin degrees of freedom using a Hartree-Fock approximation¹ on the Tight-Binding term of the Hamiltonian (3.14). One obtains two effective uncoupled Hamiltonians:

¹Using: $O_{im\sigma}^\dagger O_{jm\sigma} f_{im\sigma}^\dagger f_{jm\sigma} \rightarrow \langle O_{im\sigma}^\dagger O_{jm\sigma} \rangle f_{im\sigma}^\dagger f_{jm\sigma} + O_{im\sigma}^\dagger O_{jm\sigma} \langle f_{im\sigma}^\dagger f_{jm\sigma} \rangle$

$$\mathcal{H}_f^{eff} = - \sum_{\langle ij \rangle, m\sigma} (t_m^{eff} f_{im\sigma}^\dagger f_{jm\sigma} + h.c.) + \sum_{im\sigma} (\epsilon_m - \mu - \lambda_{m\sigma}) f_{im\sigma}^\dagger f_{im\sigma} \quad (3.15)$$

$$\mathcal{H}_S^{eff} = - \sum_{\langle ij \rangle, m\sigma} (J_m^{eff} O_{im\sigma}^\dagger O_{jm\sigma} + h.c.) + \sum_{im\sigma} \lambda_{m\sigma} \left(S_{im\sigma}^z + \frac{1}{2} \right) + \frac{U}{2} \sum_i \left(\sum_{m\sigma} S_{im\sigma}^z \right)^2 \quad (3.16)$$

These are linked to each other by the parameters of the effective hopping t_m^{eff} and the slave spin exchange constant J_m^{eff} . Both parameters and the Lagrange multipliers $\lambda_{m\sigma}$ are determined through the following self-consistency equations:

$$t_m^{eff} = t_m \langle O_{im\sigma}^\dagger O_{jm\sigma} \rangle_S \quad \forall m, \sigma \quad (3.17)$$

$$J_m^{eff} = t_m \langle f_{im\sigma}^\dagger f_{jm\sigma} \rangle_f \quad \forall m, \sigma \quad (3.18)$$

$$\langle f_{im\sigma}^\dagger f_{im\sigma} \rangle_f = \langle S_{im\sigma}^z \rangle_S + \frac{1}{2} \quad \forall m, \sigma \quad (3.19)$$

In this manner, one is left with two effective Hamiltonians: one renormalized free fermion Hamiltonian (3.15) and a spin Hamiltonian (3.16), which can be solved almost independently with coupling only through the self-consistency equations.

It is necessary to perform a further approximation to treat this model at the level of a single-site mean field. Here a random site in the lattice is considered, and embedded in the effective ‘‘Weiss mean field’’ of its surroundings (in a fashion similar to the Ising problem). The spin Hamiltonian (3.16) is then reduced to a single-site spin Hamiltonian:

$$\mathcal{H}_s = \sum_{m\sigma} (h_{m\sigma} O_{m\sigma}^\dagger + h.c.) + \sum_{m\sigma} \lambda_{m\sigma} \left(S_{m\sigma}^z + \frac{1}{2} \right) + \frac{U}{2} \left(\sum_{m\sigma} S_{m\sigma}^z \right)^2 \quad (3.20)$$

in which the mean field $h_{m\sigma}$ is determined self-consistently from:

$$h_{m\sigma} \equiv -z J_m^{eff} \langle O_{jm\sigma} \rangle = \langle O_{jm\sigma} \rangle \frac{1}{\mathcal{N}} \sum_{\vec{k}} \epsilon_{\vec{k}m} \langle f_{\vec{k}m\sigma}^\dagger f_{\vec{k}m\sigma} \rangle_f \quad (3.21)$$

where z is the coordination number of the lattice, \mathcal{N} is the number of lattice sites and $\epsilon_{\vec{k}m} = -t_m \sum_{j:n.n.(i)} e^{-i\vec{k} \cdot (\vec{r}_j - \vec{r}_i)}$ is the Fourier transform of the hopping amplitude over the sites j nearest neighbors to i . In the single site mean field approximation the renormalization of the hopping (3.17) becomes identical to the quasiparticle residue which is found to be[6]:

$$Z_{m\sigma} = \langle O_{im\sigma} \rangle^2 \quad (3.22)$$

As a result the free-fermion Hamiltonian (3.15), has its independent particles weighted by the quasiparticle residue² Z and it reads in the momentum base:

$$\mathcal{H}_f = \sum_{\vec{k}m\sigma} (Z_{m\sigma} \epsilon_{\vec{k}m} + \epsilon_m - \mu - \lambda_{m\sigma}) f_{\vec{k}m\sigma}^\dagger f_{\vec{k}m\sigma} \quad (3.23)$$

The equations (3.20, 3.21, 3.22, 3.23) and the constrain equation (3.19) self-consistently determine the parameters $h_{m\sigma}, \lambda_{m\sigma}, Z_{m\sigma}$, which completely solve the slave-spin problem.

²Also referred in this context as the *quasiparticle weight*

3.2.3 The choice of the c parameter

We discuss now how to fix the parameter c appearing in the matrix representation of the lowering operator O of equation (3.13). We ask as basic requirement of the slave-spin approximation to reproduce correctly the non-interacting limit, which is analytically solvable. Setting then $U = 0$ in equation (3.20) one demands for the quasiparticle residue to be $Z = 1$ at any given filling of the system.

In the non-interacting case all fermions are independent and one simplifies the spin Hamiltonian (3.20) to study a single electron:

$$\mathcal{H}_s = hO^\dagger + \bar{h}O + \lambda(S_\sigma^z + \frac{1}{2}) = \begin{pmatrix} \lambda & c\bar{h} + h \\ h\bar{c} + \bar{h} & 0 \end{pmatrix} \quad (3.24)$$

Working in the $S^z = \pm 1/2$ basis one has to solve a 2×2 matrix, and one finds the ground state eigenenergy and eigenstate:

$$E_{GS} = \frac{\lambda}{2} - \sqrt{\frac{\lambda^2}{4} + |a|^2} \equiv \frac{\lambda}{2} - R \quad (3.25)$$

$$|GS\rangle = \begin{pmatrix} -\frac{a}{N} \\ \frac{\lambda/2 + R}{N} \end{pmatrix} \quad (3.26)$$

Where $N = \sqrt{2R(\lambda/2 + R)}$ and $a = c\bar{h} + h$. The expected values of S^z and O are:

$$\langle S^z \rangle = -\frac{\lambda}{4R} \quad (3.27)$$

$$\langle O \rangle = -\frac{a + \bar{a}c}{2R} \quad (3.28)$$

It is clearly seen that the Lagrange multiplier λ depends on (enforces) the particle density n and, so it is adjusted to satisfy the constraint equation:

$$n - \frac{1}{2} = \langle S^z \rangle = -\frac{\lambda}{4R} \quad (3.29)$$

where c needs to be tuned to match the condition $Z = 1$

$$Z = \langle O \rangle^2 = \frac{|a + \bar{a}c|^2}{4R^2} = 1 \quad (3.30)$$

It is possible to eliminate λ from the conditions by squaring (3.29) and using the relation (3.30), following the next derivation:

$$\begin{aligned} \frac{|a|^2}{4R^2} + \left(n - \frac{1}{2}\right)^2 &= -\frac{\lambda^2}{16R^2} + \frac{|a|^2}{4R^2} \\ \frac{|a|^2}{|a + \bar{a}c|^2} &= n - n^2 \end{aligned}$$

Then it is possible to choose c real, making also h and a real. The expression for c is found to be[6]:

$$c = \frac{1}{\sqrt{n(1-n)}} - 1 \quad (3.31)$$

It is good to bring into attention that this parameter is independent of the mean field h and the Lagrange multiplier, its sole dependency is around the average particle occupation. In the half-filled case $c = 1$ and recovers the original formulation[5].

3.3 Spin-orbit Interaction

The motivation to include spin-orbit interaction arises when dealing with heavy atoms (the spin-orbit coupling $\zeta \sim Z_a^4$) and their d -orbitals of high angular momentum. A playground example, which we consider in this study, is the material Sr_2IrO_4 , whose heavy metal ion Ir^{+4} is surrounded by an Oxygen octahedron. Neglecting distortions, the electronic orbitals of the metal experience a cubic O_h symmetry and a crystal field splits the d -orbitals into an upper e_g doublet and a lower t_{2g} triplet. The crystal-field splitting between the orbitals is large compared to the Hund exchange energy. Thus the system yields a low spin state with a partially filled band, with 5 electrons occupying the Ir^{+4} t_{2g} levels and the high-energy levels e_g remaining empty. This allows to describe the system as an effective 3-orbital one. In light of experimental evidence that the material keeps the low spin state and its behavior is reduced into an effective single orbital scenario driven by the spin orbit coupling[8, 9], the Hund exchange interaction will be neglected [10] within the scope of this work.

The angular momentum operator projected into the t_{2g} levels is an effective $\ell = 1$ angular momentum operator with an extra negative sign, i.e. $P_{t_{2g}} \mathbf{L} P_{t_{2g}} = -\mathbf{L}_{\ell=1}^{eff}$. Then the spin-orbit coupling $\mathbf{L} \cdot \mathbf{S}$ leads to a further splitting into an effective pseudo total angular momentum $J_{eff} = 1/2$ doublet at an energetically higher level at $\epsilon_{J=1/2} = \zeta$ and a $J_{eff} = 3/2$ quadruplet which is at an energy level of $\epsilon_{J=3/2} = -\zeta/2$ [8, 10]. This effect arises from the negative sign of the effective angular momentum. The whole procedure is depicted on the left-hand side of figure 3.2. An alternative point of view is shown on the right-hand side of figure 3.2. In this case one first takes the action of the spin-orbit coupling in the $5d$ -orbitals, which are split into a lower energy $J = 3/2$ quadruplet and a higher energy $J = 5/2$ triplet of doublets. The crystal field action transforms this energy levels even further with a net effect once again of the $J_{eff} = 1/2$ doublet and $J_{eff} = 3/2$ quadruplet, which remain relevant at the Fermi level and the e_g levels where the orbital angular momentum is completely quenched and the spin-orbit interaction is ineffective. Hence, the effective model produced by the combined effect of the crystal field and the spin orbit is the same.

We will work then in this local diagonal basis of the pseudo total angular momentum $|j, m_j\rangle$ eigenstates and recast them into a single label α . The upper doublet with $J_{eff} = 1/2$ is therefore labeled by $\alpha = 1, 2$ with energy $\epsilon_\alpha = \zeta$ and the lower quadruplet with $J_{eff} = 3/2$ is labeled by $\alpha = 3, 4, 5, 6$ with energy $\epsilon_\alpha = -\zeta/2$. The Tight-Binding part of the Hubbard Hamiltonian (3.9), which allows hopping between lattice sites preserving orbital and spin quantum numbers, can also be directly relabeled to use the new $|j, m_j\rangle$ eigenstates as a basis. The intersite hopping amplitude t_m will be then transformed into new t_{m_j} by the $|j, m_j\rangle$ basis. For convenience sake, however, and without loss of generality, we will assume in this simple study that the t_{m_j} are all the same. Our task is understanding genuinely strongly correlated effects rising from the interplay with the spin-orbit interaction. We adopt then the simplest possible model, inspired by the comparison with a reference material like Sr_2IrO_4 , with no pretension to study its detailed characteristics. We leave to future work the study of more detailed

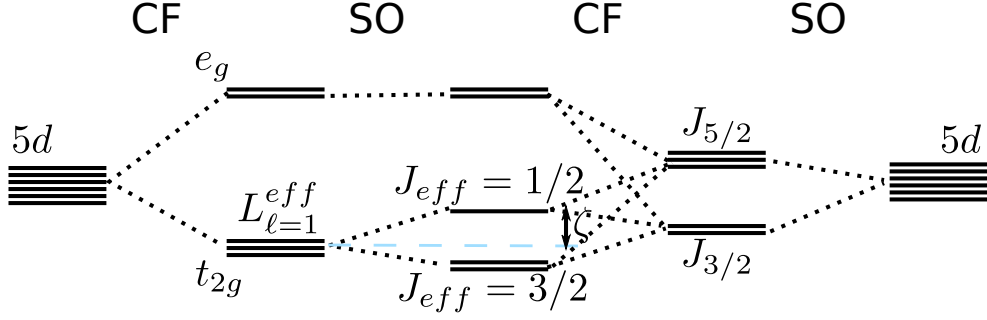


Figure 3.2: Splitting of the $5d$ energy level by the action of the crystal field(CF) and then the spin-orbit(SO) interaction(from left to center) or the splitting by the spin orbit interaction and then the crystal field(from right to center)[8]

models with precise t_{m_j} [10] which could eventually better portray the real materials. Finally the form of the local correlations term U , which describes with the total amount of charge present on a given site, does not change in the new basis $|j, m_j\rangle$, as is the same among all orbitals in our simple model. Thus one arrives into a simple model Hamiltonian

$$\mathcal{H} = \sum_{i\alpha} (\epsilon_\alpha - \mu) d_{i\alpha}^\dagger d_{i\alpha} - t \sum_{\langle i,j \rangle, \alpha} (d_{i\alpha}^\dagger d_{j\alpha} + h.c.) + \frac{U}{2} \sum_i \left(\sum_\alpha d_{i\alpha}^\dagger d_{i\alpha} - N \right)^2 \quad (3.32)$$

which is easily treatable within the slave spin mean field method of section 3.2.2.

Chapter 4

Results

Throughout this chapter, I will present the slave spin code implementation and its outcomes. There are some additional assumptions applied in this work which we have to consider. As seen in equations (3.9) and (3.32), there is no hybridization between bands, hopping preserves then the orbital quantum number. When treating the system within a local mean field, in absence of hybridization the \vec{k} dependence enters the problem only through each band dispersion as seen in equations (3.21, 3.23). Sums over momenta can thus be replaced by integrals over the energy weighted by the density of states $D(\epsilon)$, which is specific to the lattice geometry and dimension. For this work, as commonly employed in the literature, the Bethe lattice will be used. It has a very simple semi-circular form of the density of states:

$$D(\epsilon) = \frac{1}{2\pi t^2} \sqrt{4t^2 - \epsilon^2} \quad (4.1)$$

and allows to simplify calculations in a great amount. Here t is the hopping amplitude and the half-bandwidth is $D = 2t$, which is set as the energy unit throughout this work. It is known moreover that the Bethe lattice well portrays the salient physical properties of the Mott-Hubbard transition and it has immediate connection with the dynamical mean field theory[3], which is exact in the infinite dimensions limit and which we intend to implement in future work.

The mean field in equation (3.21) is then simplified into:

$$h_{m\sigma} = \langle O_{m\sigma} \rangle \int_{-\infty}^{\infty} \epsilon D(\epsilon) n_F(Z_{m\sigma}\epsilon + \epsilon_m - \mu - \lambda_{m\sigma}) d\epsilon \quad (4.2)$$

where n_F is the Fermi distribution function. In the same fashion to estimate the average particle number per site, orbital and spin, one easily uses the relation:

$$\langle n_{im\sigma} \rangle = \int_{-\infty}^{\infty} D(\epsilon) n_F(Z_{m\sigma}\epsilon + \epsilon_m - \mu - \lambda_{m\sigma}) d\epsilon \quad (4.3)$$

In this work all calculations are done at zero temperature, where the Fermi distribution can be approximated into a step function. That implies for equations (4.3) and (4.2) that:

$$Z_{m\sigma}\epsilon_{F_0}(n) = -\epsilon_m + \mu + \lambda_{m\sigma} \quad (4.4)$$

in which ϵ_{F_0} is the Fermi energy at zero temperature for the non-interacting system such that

$$\int_{-\infty}^{\epsilon_{F_0}} D(\epsilon) d\epsilon = n \quad (4.5)$$

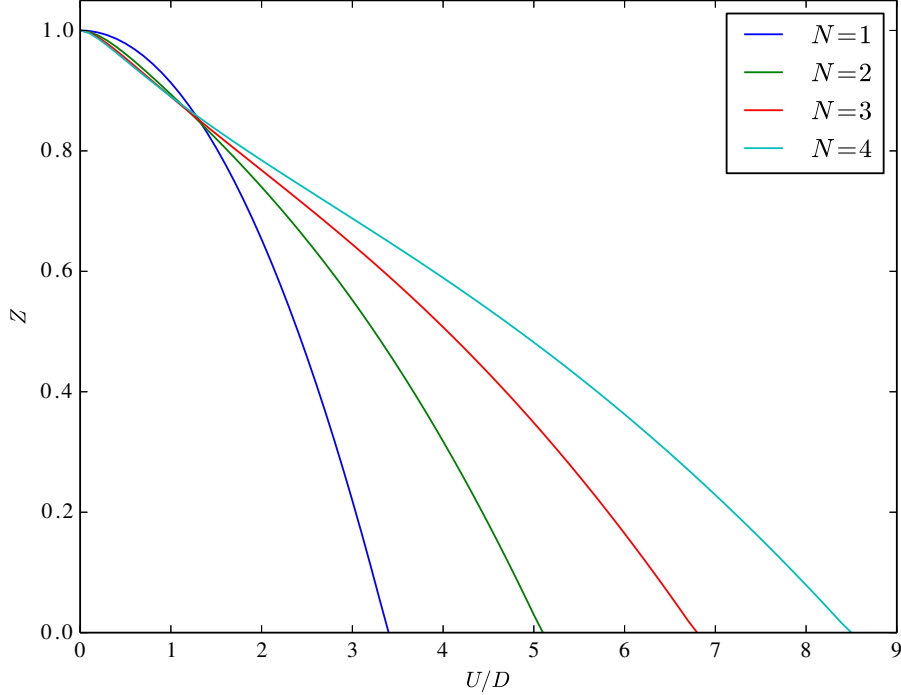


Figure 4.1: Quasiparticle weight, obtained from slave-spin mean-field for the N -orbital Hubbard Model at half-filling

This procedure of defining a zero temperature non-interacting Fermi energy ($U = 0$ and thus $Z = 1$) allows to keep the particle population fixed when correlations are included into the problem [11, 12].

4.1 Half filled multi-band case

In order to verify my own implementation of the slave spin numerical code. I reproduce the calculations presented in reference [5]. Considering systems with N degenerate orbitals, calculations over the self-consistent equations presented in section 3.2.2 are performed to study the metal-insulator transition. In this case all bands are set to the same hopping amplitude.

Without much computational effort one calculates the behavior of the multi-orbital systems at half-filling. Results are plotted in figure 4.1, where the quasiparticle weight Z is plotted as a function of the interaction parameter U/D . In this first test case one finds the expected results. Every system undergoes a transition into the insulating state, indicated by the quasiparticle weight going to zero. One sees that the greater the number of orbitals, the higher the required local coulomb repulsion U required for the system to undergo the transition into the insulating state. This plot reproduces exactly the results in reference [5]. The behavior of the algorithm is very stable, convergence to a solution of the self-consistent mean-field (3.21) and quasiparticle weight (3.22) is completely monotonic. In the case of half-filling one can profit of an additional advantage in the setup of the calculation: the chemical potential and the Lagrange multipliers, enforcing the constrain into physical states, are always zero due to the particle-hole symmetry of the Hamiltonian.

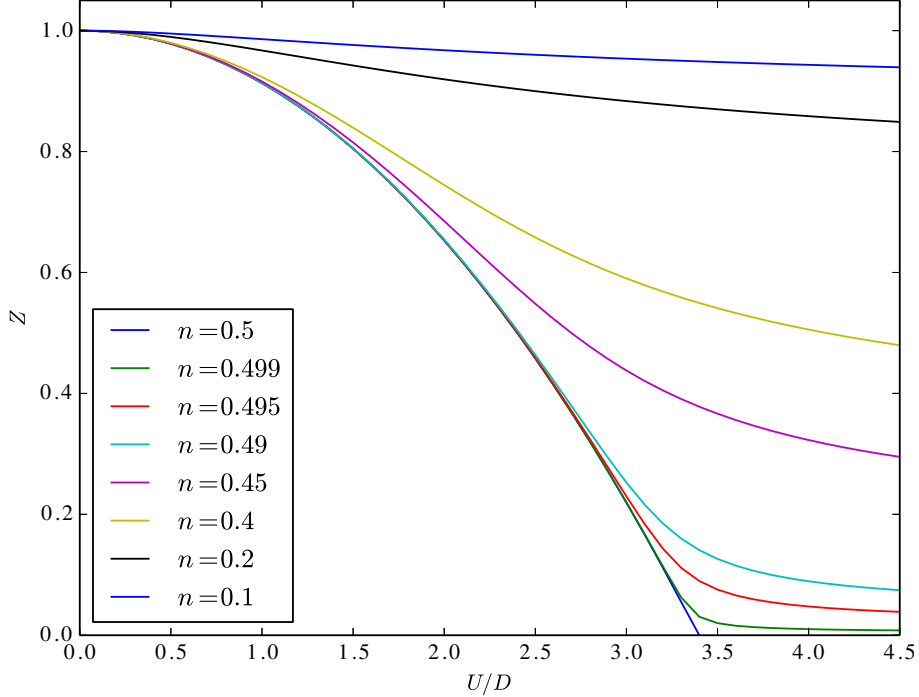


Figure 4.2: Quasiparticle weight for single band system under hole doping.

In comparison to the single band case, going to multiorbital systems is straight forward. However the implementation of the calculation code requires additional care. One of the biggest problems encountered in this first stage is how to deal with degenerate states. This poses unnoticeable problems in the single and 2 band cases when calculating the expected values of certain observables, but already in the 3 band case the issues are very drastic. One has to take special care in considering the multiplicity of degenerate eigenstates.

4.2 Doping the systems

Upon doping, Mott insulators become strongly correlated metals. This behavior can be tested within our theory by extending the previous numerical calculation code to include the new c parameter into the O operators in the spin Hamiltonian (3.20). Away from half-filling, controlling the convergence of the self-consistent equations is more difficult because the chemical potential and the Lagrange multipliers are not zero anymore by particle-hole symmetry, but they have to be determined self-consistently. The most efficient procedure which I have developed is to give the target population as input, to fix then the parameter c and find the required Fermi energy that gives the right target population using the equality (4.5). After that, one has to solve for the set of self-consistent equations given in section 3.2.2.

Results, for the single band case upon hole doping, are shown in figure 4.2 and which are in numerical agreement with the original author calculations[6]. In this figure, one can clearly see that the transition into the Mott insulating state only happens when the system is exactly populated by one electron per site, that is half filling. Upon hole-doping, the electrons can always find free sites where to move. Thus allowing them to gain in kinetic energy and keep the system metallic, though remaining strongly

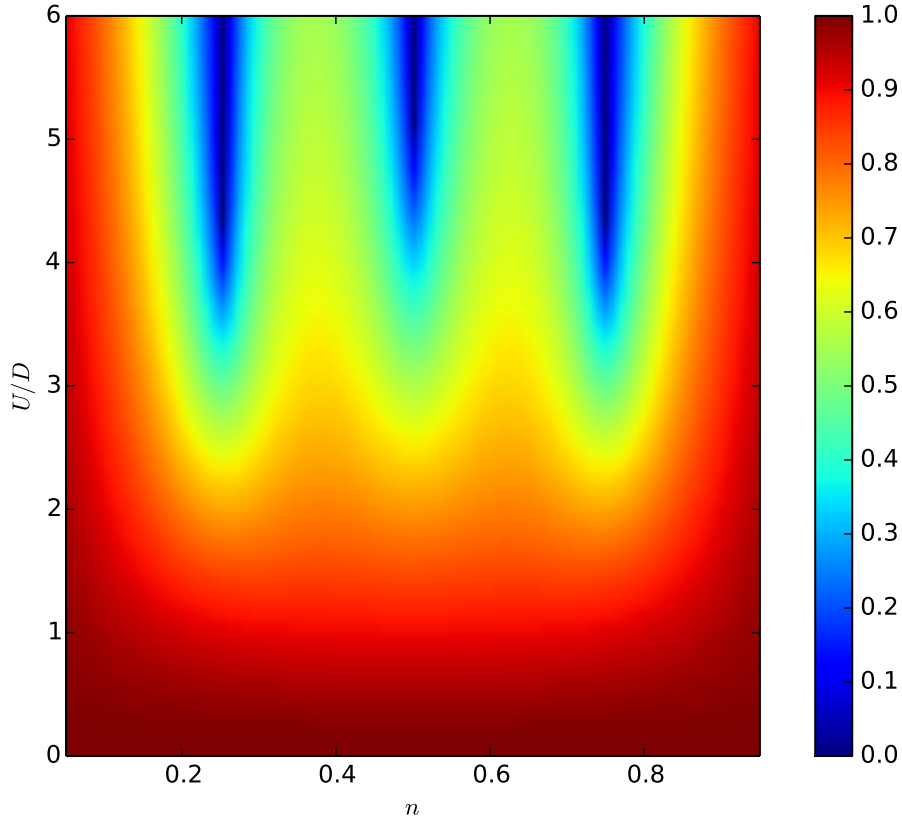


Figure 4.3: Phase diagram of the quasiparticle weight as a function of the coulomb interaction and the particle doping for a 2 orbital system.

correlated as enlightened by the small values of Z . Upon severe hole-doping the electrons behave very similar to free electrons showing very close to metallic behavior, as shown by their high quasiparticle residue, which is close to unity.

I next consider multi-orbital systems. Starting with 2 degenerate orbitals one calculates a full phase diagram of the system's behavior for the full range of doping. As one can see in figure 4.3 the system presents additional integer fillings, at which it becomes a Mott insulator. That in fact takes place for fillings of 1 or 2 or 3 electrons per site (orbital filling $n = \frac{1}{4}; \frac{1}{2}; \frac{3}{4}$). In those particular cases the system undergoes the transition from metallic into the Mott insulating state. It is also very interesting to note that the transition to the insulating state, for the cases of 1 or 3 electrons populating the site, happens at lower values of the Coulomb interaction compared to the half filled case. This is a well known behavior of the studied system as reported in reference [13].

For the 3 degenerate bands case, I only calculate the cases of integer fillings, like the case of fillings with 3 or 4 or 5 electrons per site. As shown in figure 4.4 one also sees that the transition from metal to Mott-insulator takes place and that the critical local interaction U_c is the lowest for the case of 5 electrons.

4.3 Spin orbit interaction

As specified in section 3.3, the spin-orbit interaction forces us to treat a system with non-degenerate bands. One chooses to deal with non-degenerate bands in a particular way. Using equation (4.3) properly recast to match the pseudo-total orbital angular

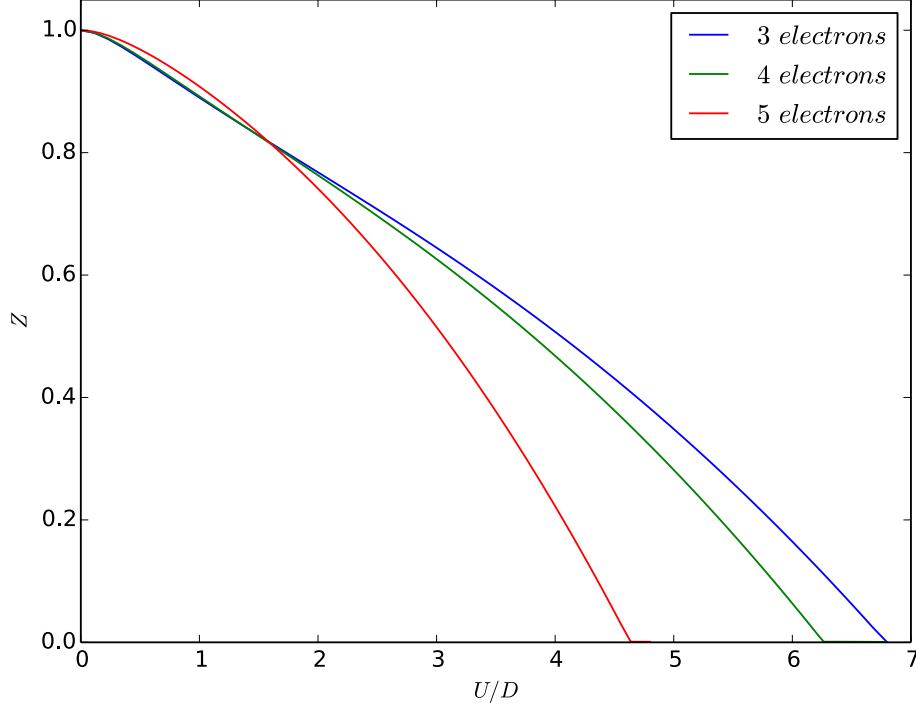


Figure 4.4: Quasiparticle weight for (3;4;5) electron systems in triple degenerate orbitals

momentum(J_{eff}) with energy band levels ϵ_α , one establishes the relation

$$\epsilon_\alpha - \mu = \lambda_\alpha - Z_\alpha \xi_\alpha(n_\alpha) \quad (4.6)$$

where $\xi_\alpha(n_\alpha)$ is the band Fermi energy¹ that gives the desired band filling n_α in the free system($U = 0$). From here on, one can define the energy separation between band centers as:

$$\Delta = (\epsilon_2 - \mu) - (\epsilon_4 - \mu) = (\lambda_2 - \lambda_4) - (Z_2 \xi_2 - Z_4 \xi_4) \quad (4.7)$$

where the indexes 2 and 4, correspond to the energy levels of the $J_{eff} = 1/2$ upper doublet and the lower quadruplet with $J_{eff} = 3/2$. In this fashion, the strength of the spin-orbit interaction(ζ) is included in our calculations by the relation:

$$\Delta = \epsilon_2 - \epsilon_4 = \frac{3}{2}\zeta \quad (4.8)$$

From now on, one solves all the self-consistent equations proposed in section 3.2.2. To keep account of the spin-orbit interaction strength(ζ) the previous relation (4.8) is enforced as a constrain. When the local Coulomb interaction is raised ($U > 0$) band populations will be self-consistently exchanged as to satisfy equation (4.7). That is to say different electron population combinations are set up in each band to satisfy the global population (5 electrons) and calculate the band Fermi energies in the $U = 0$ case, those values are held fixed at $U > 0$ and one verifies if equation (4.7) is fulfilled. The output of this calculations is presented in the phase diagram shown in figure 4.5, where one identifies 3 main phases.

¹For numerical reasons due to the expression of the algorithm, it is simpler to set the band occupation of each band individually by using a different Fermi energy in each band.

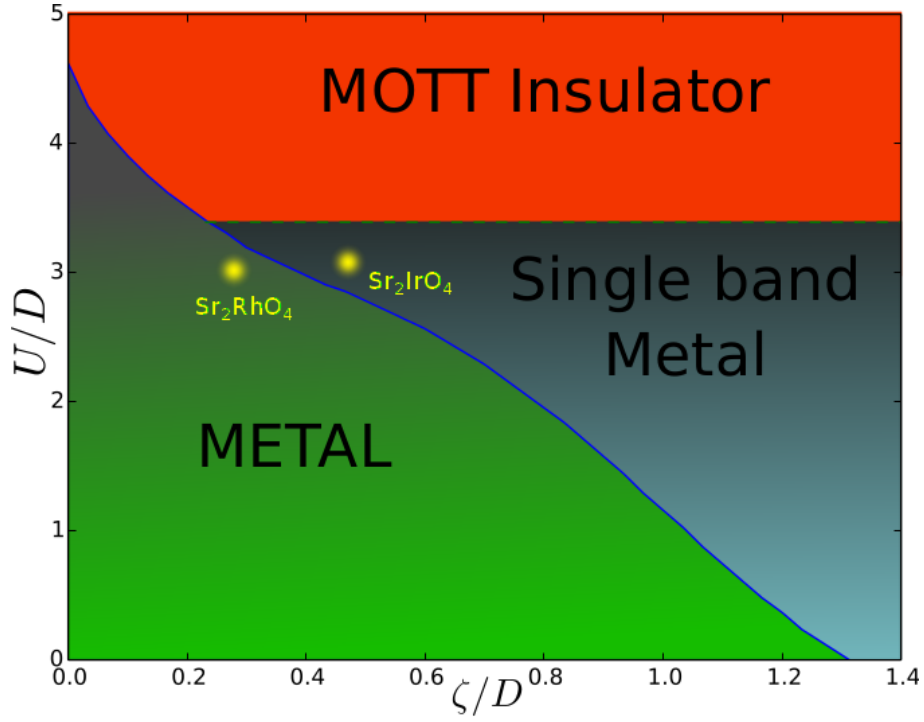


Figure 4.5: Phase diagram for a 3 orbital system populated by 5 electrons, where spin-orbit interaction and electronic correlations are taken into account

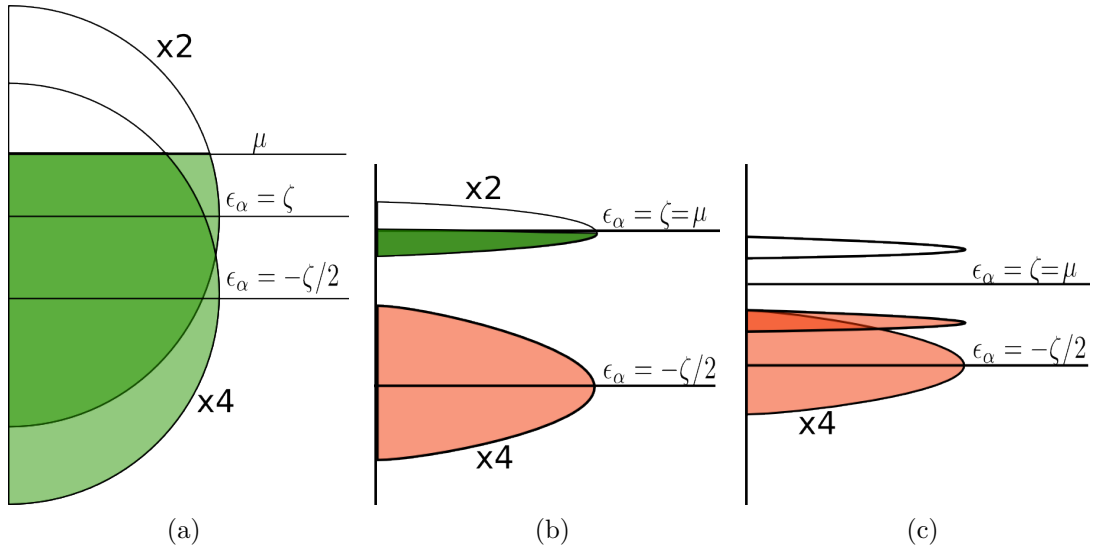


Figure 4.6: Schematic illustration of the behavior of the different bands in each of the phases: a) Metallic phase: all bands overlap and are partially filled. b) Single band metal: lower $J_{eff} = 3/2$ quadruplet is filled to form a band insulator, remaining upper doublet is half-filled. c) Spin-orbit assisted Mott insulator: upper $J_{eff} = 1/2$ doublet forms upper and lower Hubbard bands.

The Metallic state is situated into the lower left corner of the phase diagram where the electronic correlations and the spin-orbit coupling are both low. In this case all bands remain partially filled allowing for conducting states as illustrated in figure 4.6a. Correlations reduce the effective bandwidth of the quasiparticles, thus bands change their filling levels accordingly. At the low spin-orbit interaction region ($\zeta/D < 0.23$) both bands ($J_{eff} = 3/2$ and $J_{eff} = 1/2$) tend to shrink proportionally, thus the migration of electrons between bands is mild until those effective bandwidths are comparable to the spin-orbit splittings. At that point there is a rushed migration of electrons into the lower band, filling it completely and terminating the metallic phase. Figure 4.7 shows this occupation migration out of the upper band. Intermediate and strong values of the spin-orbit interaction ($\zeta/D > 0.23$) induce a more severe transfer of electrons into the lower band as soon as the local Coulomb interaction is raised (figure 4.7), because the electronic bandwidths are unevenly reduced and more distant in the energy scale.

The Effective single band Metal follows from the metallic state as correlations are raised and the spin-orbit splitting is large enough ($\zeta/D > 0.23$) compared to the effective bandwidths. In this case bands will not overlap anymore on the energy axes (illustration in figure 4.6b). The lower band at $J_{eff} = 3/2$ becomes completely filled and thus it becomes an insulating valence band. The higher energy band, at $J_{eff} = 1/2$, remains half-filled and not too reduced in bandwidth so it shows a correlated metal behavior, conducting states are only allowed in this band.

Spin-orbit assisted Mott Insulator If correlations are strong enough the lower Hubbard band and upper Hubbard band may form in the $J_{eff} = 1/2$ band after the lower band at $J_{eff} = 3/2$ is completely filled. The system is driven then to the Mott insulating state since the lower Hubbard band becomes also completely filled, as illustrated in figure 4.6c. This transition happens abruptly from the metallic state for low values of spin-orbit coupling ($\zeta/D > 0.23$), here the electronic correlations are already higher than those required to drive a half-filled single band system into the insulating state. For larger values of spin-orbit interaction ($\zeta/D > 0.23$), the system transitions smoothly from the metallic phase into effective single band metallic behavior and then into the Mott insulating state as correlation are increased in this effective single band.

To further justify the found phases and statements, I include plots of the quasiparticle residue of the upper $J_{eff} = 1/2$ band in figure 4.8 and of the lower band $J_{eff} = 3/2$ in figure 4.9. The quasiparticle residue is responsible for the effective reduction of the bandwidths in the free fermion Hamiltonian (3.23). The limit cases are also included, as the case of no spin-orbit interaction where one has the behavior of a 5 electron system in 3 degenerate bands and also the half-filled single band scenario. At low spin-orbit interaction ($\zeta/D = 0.03$), the quasiparticle residue in both cases (upper and lower bands) is very similar to the degenerate case but it separates from it when the band populations change abruptly. Once the system has the lower bands completely filled, the band insulator case, the upper band is half-filled behaving like a single band and in this case it experiences a Coulomb interaction larger than the one needed to transition into the Mott insulating state in the single band case, so the Mott insulating state is established. This behavior of a sharp phase transition of a spin-orbit assisted Mott

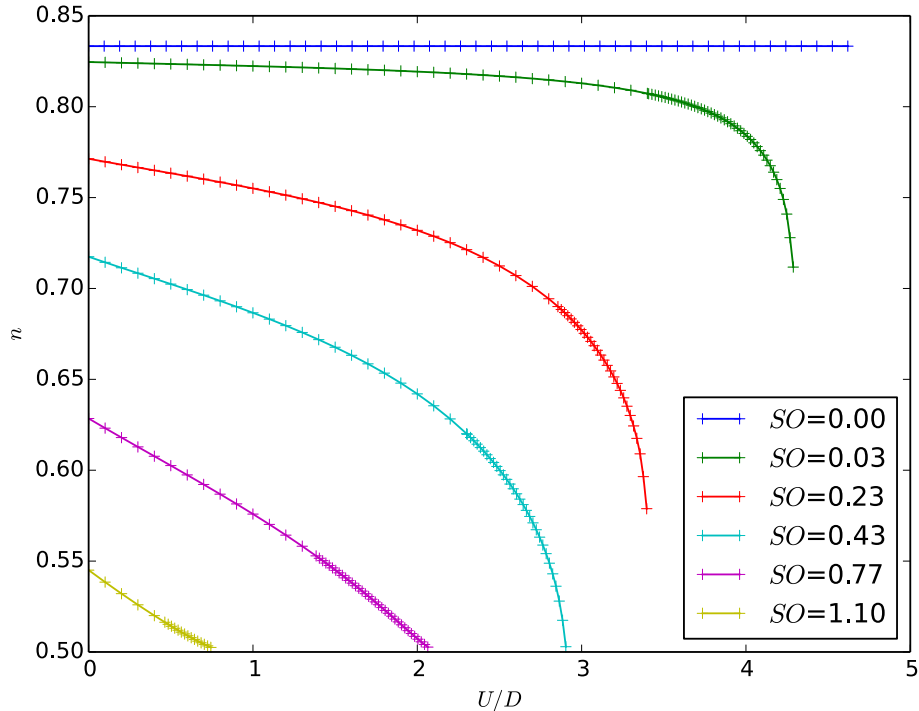


Figure 4.7: Electronic occupation change of the upper doublet as a function of the local Coulomb interaction U , for different strengths of the spin-orbit interaction ($SO = \zeta/D$).²

insulator is continued for the low values of spin-orbit interaction ($\zeta/D < 0.23$). For larger values of the spin-orbit interaction, the quasiparticle weight of the upper band and lower band differ from each other in greater amounts. The upper band shows a faster drop in its quasiparticle weight (figure 4.8) up to the case that it actually follows the behavior of a half-filled single band, this shows that the system is indeed reduced into an effective single band Hubbard model[8]. On the other hand, the quasiparticle weight behavior in the lower band tends to maintain its similitude to the degenerate 3-band 5-electron system.

We now try to interpret this spin-orbit assisted Mott transition by comparing with real materials parameter. Converting the parameters values used for band structure calculations in 2 specific materials[14] (Sr_2IrO_4 and Sr_2RhO_4) to the normalized unit system of our model, I mark them into the phase diagram of figure 4.5. For the case of Sr_2IrO_4 , the material around which the model was developed, our results locate it in the single band metallic phase close to the insulator transition. The real material behavior is indeed reduced to an effective single band case but as a matter of fact it is already an insulator[8]. The material Sr_2RhO_4 is placed in the metallic phase and cannot be treated as a single band system, which is in complete agreement with the real material behavior.

The elaborated simple model is capable of describing the cooperative action of the spin-orbit interaction with the electronic correlations to drive systems insulating through the formation of an effective single band system. Despite the strong simplifi-

²For numerical reasons, limited by the expression of the c parameter (3.31), it is impossible to perform any calculation when the lower band is filled or very close to it. For this reason the plots, presented further on, display terminated curves. The reader is expected to continue the curves in plot towards half-filling.

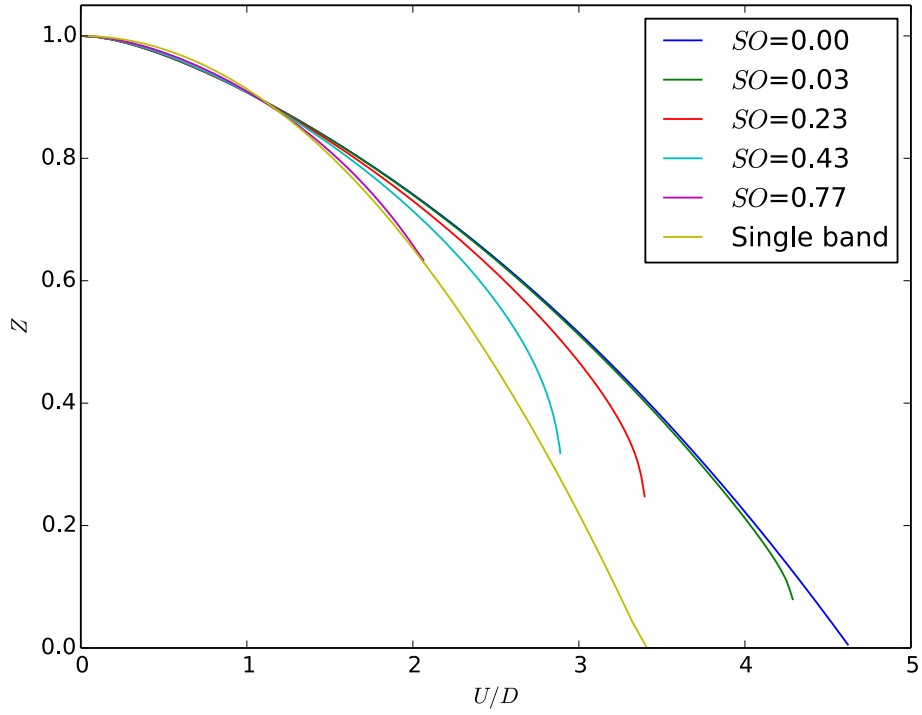


Figure 4.8: Quasiparticle weight of the upper doublet $J_{eff} = 1/2$

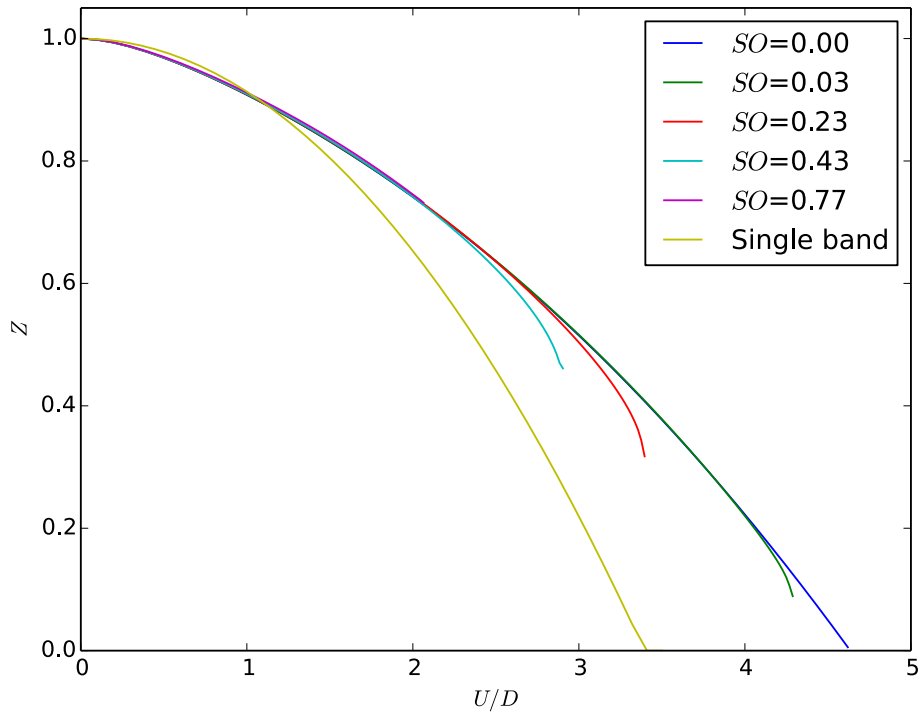


Figure 4.9: Quasiparticle behavior at the lower quadruplet $J_{eff} = 3/2$

cations in our modeling, like giving all bands equal bandwidths and omitting the real lattice geometry, the out-coming calculations are still able to qualitatively recover the behavior of the real materials.

4.4 Weaknesses of the method

The slave-spin mean field theory is successful to recover known physical results in the domain of strongly correlated electrons systems. Its numerical algorithm provides ease of use and it is computationally inexpensive, this allows for the possibility of performing multiple calculations with many different parameters and map entire phase diagrams in little time, as done in this study. Nevertheless, one also needs to criticize the limits of this method and the set of problems that come with it.

In this method, one has to work at zero temperature where the Fermi distribution is taken as a step function and there is a sharp cut in the occupied states forming the ground state. When treating our slave spin theory at finite temperatures, the temperature itself becomes ill defined because it cannot be held equivalent between the fermion and spin systems. Another constrain of the method is that the Mott insulating state, where the quasiparticle weight is zero implies as well that the spin mean field is zero as well. A null spin mean field is a strong solution of the slave-spin formulation. Thus, once an insulating case is encountered, the self-consistent equations are fulfilled and the system will not leave such state under the change of setup parameters alone. For this reason it is only possible study the transition from the metallic phase into the insulating one, and not the other way around so to explore the coexistence regions and develop hysteresis loops of the metal to Mott insulator transition.

The inclusion of the c parameter allows to use this slave particle technique away of half-filling and it is good enough since it is capable of reproducing very well know physical cases. Despite of that, I want to bring into memory the relation (3.27), where one recognizes the work of the Lagrange multiplier (λ). λ does not only enforce the constrain (3.19) to keep the fluctuations/behavior in the extended Hilbert spaces around real states. It acts as a magnetic field promoting a certain magnetization of the extended slave spin system. That is required because equation (3.29) relates the average fermion populations with the “magnetization” in the extended spin system. This is accomplished without any trouble in the calculations for the degenerate orbitals case and the use of the remark of relation (4.4) greatly facilitates the work.

Nonetheless, when dealing with non-degenerate orbitals, as required by the model Hamiltonian to include the spin-orbit interaction (equation (3.32)), a new set of problems arise. The very same action of the Lagrange multiplier promoting a magnetization in the spin system and that it is orbital selective makes it impossible to fulfill the relation (4.4), and obtain the right orbital populations using a unique chemical potential μ . The first check, is always to solve the free system ($U = 0$) where the analytical solution is known. But there one cannot link anymore the values of the orbital energy and the chemical potential of the real system to the ones into the free fermion Hamiltonian (3.23), even when in the free case they are theoretically by construction the same. For such correspondence to match, one needs the Lagrange multipliers to be zero, but they are not away of half-filled degenerate bands as declared by equations (3.29) and (3.27). A solution can be obtained by assigning to each orbital a different chemical potential, in this way relation (4.4) is fulfilled up to an orbital specific chemical potential and

the orbital fillings acquire the right values as declared for the free case analytic solution. But how to choose then the good chemical potentials and orbital populations once interactions are included ($U > 0$)?

This problematic remains partially hidden in the literature [15], new attempts to fix the problem do not get much improved results [16, 17]. To the current state of our knowledge the problem remains unsolved. All the series of approximations proposed to make the problem treatable also induce a bias on how the output calculation will turn out to be. I also tried new personal methods, which are discussed in the appendix, but results were not satisfactory enough.

Chapter 5

Conclusions and future work

In this work, for the case of a 5 electron system in 3 bands, it was shown that spin-orbit coupling tends to cooperate with Coulomb interaction to enhance the degree of electron correlations and produce spin-orbit assisted Mott insulators, as the required critical Coulomb interaction (U_c) to render the system insulating is reduced.

The proposed simple model presents qualitatively good correspondence with the real materials properties, like Sr_2IrO_4 and Sr_2RhO_4 . The investigation of correlated systems with strong spin-orbit coupling is still in its early development, and there are rapid theoretical developments and experimental research in this area. There are still many scenarios to consider and phases to explore. As most obvious are the inclusion of electron/hole doping into the system, to recover metallic states (there is also a search into High-Tc superconductivity[2]). One has to include the geometrical lattice structure to review effects on the electronic bands and topological phases. One needs to calculate over clusters of lattice sites, to explore the magnetic phases as to include corrections to the single site approximation considered in this work. As further work one can include the Hund's coupling, which is at the same energy scale to the spin-orbit interaction[14] and plays a great role in multi-orbital systems[18, 19, 15]. It is excluded in this work based on the fact that Sr_2IrO_4 , our playground system, is in a low spin state[10] and that the system is reduced into as a single band case[8, 9] where only the spin-orbit effect is relevant. The Hund's coupling may be however important in other systems.

On the theoretical and methodological side, the slave spins method can still be improved. At the late development of this work, new personal ideas arose to modify the representation of slave spins which are still worth trying in order to test for the *same/different/new* results in the calculations. There is as well the need to use more advanced techniques like the DMFT[3]. The DMFT is a method to treat strong correlations and I would like to develop the spin-orbit interaction within this method.

Bibliography

- [1] M. Imada, A. Fujimori, and Y. Tokura, “Metal-insulator transitions,” *Rev. Mod. Phys.*, vol. 70, pp. 1039–1263, Oct 1998.
- [2] W. Witczak-Krempa and G. Chen, “Correlated quantum phenomena in the strong spin-orbit regime,” *arXiv preprint arXiv: ...*, 2014.
- [3] A. Georges, G. Kotliar, W. Krauth, and M. Rozenberg, “Dynamical mean-field theory of strongly correlated fermion systems and the limit of infinite dimensions,” *Reviews of Modern Physics*, vol. 68, no. 1, 1996.
- [4] A. J. M. S. Dresselhauss, G. Dresselhauss, *Group Theory: Application to the physics of Condensed Matter*. Springer-Verlag Berlin Heidelberg, 2008.
- [5] L. De’Medici, A. Georges, and S. Biermann, “Orbital-selective mott transition in multiband systems: Slave-spin representation and dynamical mean-field theory,” *Physical Review B*, vol. 72, no. 20, p. 205124, 2005.
- [6] S. Hassan and L. De’Medici, “Slave spins away from half filling: Cluster mean-field theory of the hubbard and extended hubbard models,” *Physical Review B*, vol. 81, no. 3, p. 035106, 2010.
- [7] De’Medici, *Aspects sélectifs en orbitales de la transition metal-isolant de Mott*. PhD thesis, École Polytechnique, 2006.
- [8] B. Kim, H. Jin, S. Moon, J.-Y. Kim, B.-G. Park, C. Leem, J. Yu, T. Noh, C. Kim, S.-J. Oh, J.-H. Park, V. Durairaj, G. Cao, and E. Rotenberg, “Novel $J_{eff} = 1/2$ Mott State Induced by Relativistic Spin-Orbit Coupling in Sr_2IrO_4 ,” *Physical Review Letters*, vol. 101, p. 076402, Aug. 2008.
- [9] B. Kim, H. Ohsumi, T. Komesu, and S. Sakai, “Phase-sensitive observation of a spin-orbital Mott state in Sr_2IrO_4 ,” *Science*, vol. 323, no. March, pp. 1329–1332, 2009.
- [10] D. Pesin and L. Balents, “Mott physics and band topology in materials with strong spin-orbit interaction,” *Nature Physics*, vol. 6, pp. 376–381, Mar. 2010.
- [11] R. Yu and Q. Si, “Mott transition in multiorbital models for iron pnictides,” *Physical Review B*, vol. 84, p. 235115, Dec. 2011.
- [12] S. Florens and A. Georges, “Slave-rotor mean-field theories of strongly correlated systems and the Mott transition in finite dimensions,” *Physical Review B*, vol. 70, p. 035114, July 2004.

- [13] M. J. Rozenberg, “Integer-filling metal-insulator transitions in the degenerate Hubbard model,” *Physical Review B*, vol. 55, pp. R4855–R4858, Feb. 1997.
- [14] C. Martins, M. Aichhorn, L. Vaugier, and S. Biermann, “Reduced effective spin-orbital degeneracy and spin-orbital ordering in paramagnetic transition-metal oxides: Sr_2IrO_4 versus Sr_2RhO_4 ,” *Physical review letters*, pp. 4–8, 2011.
- [15] L. de’ Medici, S. Hassan, M. Capone, and X. Dai, “Orbital-Selective Mott Transition out of Band Degeneracy Lifting,” *Physical Review Letters*, vol. 102, p. 126401, Mar. 2009.
- [16] R. Yu and Q. Si, “U(1) slave-spin theory and its application to Mott transition in a multiorbital model for iron pnictides,” *Physical Review B*, vol. 86, p. 085104, Aug. 2012.
- [17] A. Rüegg, S. D. Huber, and M. Sigrist, “Z₂-slave-spin theory for strongly correlated fermions,” *Physical Review B*, vol. 81, p. 155118, Apr. 2010.
- [18] P. Werner and A. J. Millis, “High-Spin to Low-Spin and Orbital Polarization Transitions in Multiorbital Mott Systems,” *Physical Review Letters*, vol. 99, p. 126405, Sept. 2007.
- [19] L. de’ Medici, J. Mravlje, and A. Georges, “Janus-faced influence of hund’s rule coupling in strongly correlated materials,” *Phys. Rev. Lett.*, vol. 107, p. 256401, Dec 2011.

Appendix A

Slave spin method modifications

In my own contribution to treat the undesired behavior of the slave spin mean field approximation, I enforced certain changes. My first attempt was not to follow the direct representation change $d^\dagger d \rightarrow f^\dagger f$ for the local number operators, but use the full representation change $d^\dagger d \rightarrow O^\dagger O f^\dagger f$. Then still enforcing the original constrain (3.2), this would change the coupled Hamiltonians into:

$$\mathcal{H}_s = \sum_{m\sigma} (h_{m\sigma} O_{m\sigma}^\dagger + h.c.) + \sum_{m\sigma} \left[n_{m\sigma} O_{m\sigma}^\dagger O_{m\sigma} + \lambda_{m\sigma} \left(S_{m\sigma}^z + \frac{1}{2} \right) \right] + \frac{U}{2} \left(\sum_{m\sigma} S_{m\sigma}^z \right)^2$$

$$\mathcal{H}_f = \sum_{\vec{k}m\sigma} [Z_{m\sigma} (\epsilon_{\vec{k}m} + \epsilon_m - \mu) - \lambda_{m\sigma}] f_{\vec{k}m\sigma}^\dagger f_{\vec{k}m\sigma}$$

In this case the parameter c (to be tuned away of half-filling) has to be numerically found, as it has no simple analytical expression. The advantages of this first modification are that the c parameter remains symmetric to hole or electron doping and is closer to unity in wider range around half-filling than the expression (3.31). It also drops the values of the Lagrange multipliers closer to zero, but still non-zero. The quasiparticle residue weights not only the band dispersion but the orbital energy and chemical potential which becomes helpful when assigning the orbital populations. On its downsides there is an asymmetric behavior of the Lagrange multiplies and the chemical potential depending on hole or electron doping, giving very high values in magnitude after substantial electron doping ($n > 0.7$). The next step was to enforce the constrain to couple the spin and fermion representation like $O^\dagger O f^\dagger f = S^z + 1/2$ in this case solutions could only be found in the range $n \in (0; 0.56)$, rendering this approach useless for larger n .

On a different attempt, after the first version of this work was completed, I developed a new structure for the generic spin operator (equation (3.13)). Its expression is searched for after the single site approximation is done and by keeping the requirement that it is unitary ($O^\dagger O = 1$) at any given doping. The new found form reads in the $S^z = \pm 1/2$ basis:

$$O = \begin{pmatrix} 2n - 1 & 2\sqrt{n - n^2} \\ 2\sqrt{n - n^2} & 1 - 2n \end{pmatrix} \quad (\text{A.1})$$

This new operator comes with the advantages that: it is well defined for all band fillings (empty and full cases included), the Lagrange multipliers are zero and the quasiparticle weight is unity in the free case ($U = 0$) while respecting the orbital populations of the analytical solution. At half-filling it recovers the shape of the well defined operator, for the slave spin approximation. Results on the doped single band case are indistinguishable from reference [6] in the range $n \in (0.4; 0.6)$ and on higher doping the results are well behaved. Despite all this advantages this new operator is not enough, it is not be able to capture the transition into the Mott insulator at any integer filling in multi-orbital systems, only the half-filled case becomes insulating. As such this approach becomes again insufficient when dealing with multi-orbital systems.